

Wind-induced vibration control of a 200 m-high tower-supported steel stack

Tatsuya Susuki[†] and Naoya Hanada[‡]

Civil Engineering Department, Kyushu Electric Power Co., Inc., Fukuoka 810-8720, Japan

Shin Homma[‡]

Steel Structures Headquarters, Hitachi Zosen Corporation, Osaka 550-0002, Japan

Junji Maeda^{‡†}

Faculty of Human-Environment Studies, Kyushu University, Fukuoka 812-8581, Japan

(Received February 27, 2006, Accepted July 18, 2006)

Abstract. It is well known that cylinder steel stacks are heavily impacted by vortex-induced vibration. However, the wind-induced vibration behaviors of tower-supported steel stacks are not clarified due to a lack of observation. We studied a stack's response to strong winds over a long period of time by observing the extreme wind-induced vibration of a 200 m-high tower-supported steel stack. This experiment aimed to identify the wind-induced vibration properties of a tower-supported steel stack and assess the validity of the vibration control method used in the experiment. Results revealed a trend in wind-induced vibration behavior. In turn, an effective measure for controlling such vibration was defined by means of increasing the structural damping ratio due to the effects of the tuned mass damper to dramatically decrease the vortex-induced vibration of the stack.

Keywords: tower-supported steel stack; strong wind observation; vortex-induced vibration; damping ratio.

1. Introduction

The stacks of thermal power plants may reach up to 200 m in height. This height regulation was mandated for power generation functions and environmental conservation. At such extreme heights, the stacks, which have a large aspect ratio, are susceptible to the impact of strong winds. In particular, it is known that stacks having circular cross sections are stringently required appropriate designs against vortex-induced vibration (Simiu and Scanlan 1996, Vickery 1998, Koten 1998). Given this situation, many observations of the response of cylinder-type stacks to strong winds were

[†] Senior Engineer, Corresponding Author, E-mail: tatsuya.susuki@san.bbiq.jp

[‡] Senior Engineer

^{‡†} Professor

reported (Ciesielski, *et al.* 1992, Sanada, *et al.* 1992); and, several standards for stack design were also proposed in the past (Eurocode 1 1995, CICIND 1999). The stack's damping ratio has a significant impact on the development of vortex-induced vibration; therefore, studies comparing the observed values with standard values have been conducted (Verwiebe and Berger 1999). In addition, various countermeasures against the outbreak of vortex-induced vibrations on actual stacks have been reported (Ueda, *et al.* 1992, Tranvik and Alpsten 2005).

In turn, ultra-high stacks supported by a truss-structured steel tower are expected to have more complicated vibration properties due to their shape (Architectural Institute of Japan 1996). However, a few reports of wind response observations of actual stacks (Kawamura, *et al.* 1992, Kawamura and Okazaki 1999) are insufficient for the clarification of their minute dynamic behaviors. At Kyushu Electric Power, vibration of a 200 m-high tower-supported steel stack was seen under strong winds. In response, the authors conducted an observation of the wind responses of an ultra-high stack built in the Kyushu area of Japan (Makihata, *et al.* 2002, Homma, *et al.* 2004, Susuki, *et al.* 2004). Further, a man-powered vibration test and a wind tunnel test were conducted to analyze the phenomena occurring on the actual stack under observation (Homma, *et al.* 2004). This paper reports the wind-induced vibration properties as seen in the response of a 200 m-high tower-supported steel stack built in northern Kyushu, in the period from 2000 to 2003. Particular focus was placed on the change in damping ratio and the vibration depression efficiency due to the installation of a tuned mass damper (TMD) vibration control device at the top of the tower as well as the relationship between the damping ratio and the wind response of the tower.

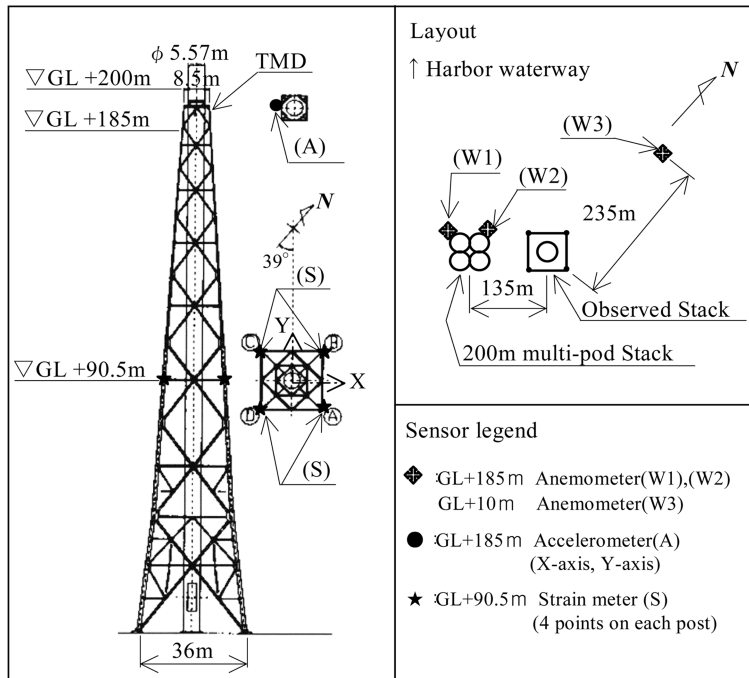


Fig. 1 Outline of observed stack

Table 1 Structural specifications of observed stack

Location	Kitakyushu City, Fukuoka Prefecture
Completion	1982
Use	LNG-fired thermal power plant
Type	Single-stack shell, four-post, tower-supported type
Stack shell outer diameter	$\phi 5.57$ m
Stack shell height	GL+200 m
Tower width	Base: 36 m, top: 8.5 m
Tower height	GL+185 m
Main material	SS400 (JIS G 3101), STK400 (JIS G 3444)
Member connection	Weld bonding for stack shell and tower post, high strength bolt connection for other members
Stack shell support	Supported in a horizontal direction at 8 points with no constraint in the vertical direction
Remarks	Mortar type lining inside the stack shell

2. Observations

2.1. Stack structure and observation items

A sketch of the observed stack is shown in Fig. 1; and, the structural specifications of the observed stack are shown in Table 1. The stack faces the harbor waterway in the north to west directional range. Various medium-rise buildings, including the power plant building, occupy the other directions. Thus, winds from the northerly to westerly directions are sea breezes and those from other directions are land breezes. The 200 m-high multi-pod stack is lined up 135 m southwest of the observed stack. The authors collected data in three categories: wind direction and speed using three anemometers, the stack's vibration acceleration using two accelerometers, and the stack's strain using sixteen strain meters. For wind direction and speed, wind at GL+10 m was registered by the ultrasonic anemometer W3 located inside the power plant premises 235 m away from the observed stack; and, wind at GL+185 m was registered by the propeller anemometers W1 and W2 installed on the aligned stack. To see how the stack's vibration accelerates, measures of the vibration of the whole stack structure were obtained with the accelerometer *A* (X-axis, Y-axis) at GL+185 m. The stack's strain data was obtained with a strain meter *S* located at four points on each post at GL+90.5 m.

The time periods of the observation, which was segmented into three stages, are shown in Table 2. In stage 1, no vibration control was installed. While in stages 2 and 3, a TMD with various damping ratios was installed in order to examine individual vibration properties.

Table 2 Observation periods and conditions of each stage

Observation stage	Time period	Conditions
1	Aug. '00 - Dec. '01	No vibration control device
2	Dec. '01 - May '02	TMD installed
3	May '02 - Mar. '03	TMD installed (after adjustment)

2.2. Observation data storage and analysis

Observation was conducted on a continuous basis; and, the data was categorized in two ways, as follows:

- a. Fixed time observation: 10 minutes before every hour in 10-minute units
- b. Continuous observation: upon occurrence of either an instantaneous wind speed of 14 m/s or more, or a vibration acceleration of 120 Gal or more at $GL+185$ m in 10-minute units

The wind direction and speed data were used to analyze the wind conditions, including trends in wind direction and speed, as well as gust factor $GF_w (= U_{\max}/U_{\text{mean}})$. Here, U_{\max} is the maximum instantaneous wind speed at 10 min/unit, and U_{mean} is the average wind speed at 10 min/unit. The stack's vibration acceleration data was used to analyze the occurrence of the stack's vortex-induced vibration (vibration at a right angle against the wind direction) as well as the correlation between the wind direction and speed and the vortex-induced vibration. Similarly, the stack's strain data was used to analyze the stack's gust response (response in the direction of the mean wind) as well as the correlation between the wind direction and speed and the gust response. The natural frequency and damping ratio of the stack were also employed to examine vortex-induced vibration and gust response, respectively. In the study described in this paper, we employed either value without including any impact from structures among the values of the wind direction and speed obtained at W1 and W2.

3. Observation results

3.1. Wind conditions and stack vibration properties

The wind conditions from Stages 1-3 are shown in Table 3. The exponent α that indicates the vertical distribution of the wind speed is defined as $U_{185} = U_{10}(185/10)^\alpha$. Here, U_{10} and U_{185} are 10-minute average wind speeds obtained at $GL+10$ m and $GL+185$ m, respectively. The figures suggest that the prevailing wind direction in the region is east; however, westerly winds prevail in winter.

Table 4 shows the damping ratio obtained in each stage as well as the resonant velocity of the

Table 3 Wind condition

Direction	Stage 1		Stage 2		Stage 3	
	Exponent α	Occurrence rate (%)	Exponent α	Occurrence rate (%)	Exponent α	Occurrence rate (%)
N	0.235	10.7	0.228	8.4	0.185	11.7
NE	0.244	11.1	0.229	9.5	0.215	10.0
E	0.238	26.2	0.265	19.0	0.357	24.9
SE	0.339	11.6	0.333	6.9	0.344	10.7
S	0.328	6.5	0.267	5.7	0.276	10.0
SW	0.187	11.9	0.225	13.6	0.229	14.9
W	0.248	12.8	0.229	20.0	0.245	13.9
NW	0.157	9.4	0.309	17.0	0.192	3.9

Table 4 Damping ratio and resonant velocity

Stage	Damping ratio (%)	Natural frequency (Hz)	Resonant velocity (m/s)	
			$U_{2H/3}$ *1	U_{185} *2
1	0.33	0.56	17.3	18.5
2	0.89	0.53	16.4	17.5
3	4.00	0.54	16.7	17.8

*1 $U_{2H/3} = f \cdot D / S_i$; H : stack height (200 m) D : stack shell diameter ($\phi 5.57$ m) S_i : Strouhal number (0.18).

*2 $U_{185} = U_{2H/3} (185/133.3)^\alpha$ $\alpha = 0.20$ (Average value of observation data).

vortex-induced vibration calculated from the stack’s natural frequency. The damping ratios in Stages 1 and 3 were derived from the free damped vibration waveform in a man-powered vibration test at $GL + 185$ m. The value in Stage 2 was based on the wind response waveform, applying the RD method. The value in Stage 1 is smaller than 0.5%, or the damping ratio of the usual stacks lined with refractory concrete (CICIND 1999). The damping ratio increased from 0.33% in Stage 1 to 4% in Stage 3, demonstrating a decrease in the stack’s wind response due to the effect of the TMD.

3.2. Vortex-induced vibration based on vibration acceleration data

The correlation between U_{185} and the vibration acceleration data for each stage is shown in Fig. 2. Each plot uses the average value calculated for each block of stored data. The figure indicates the

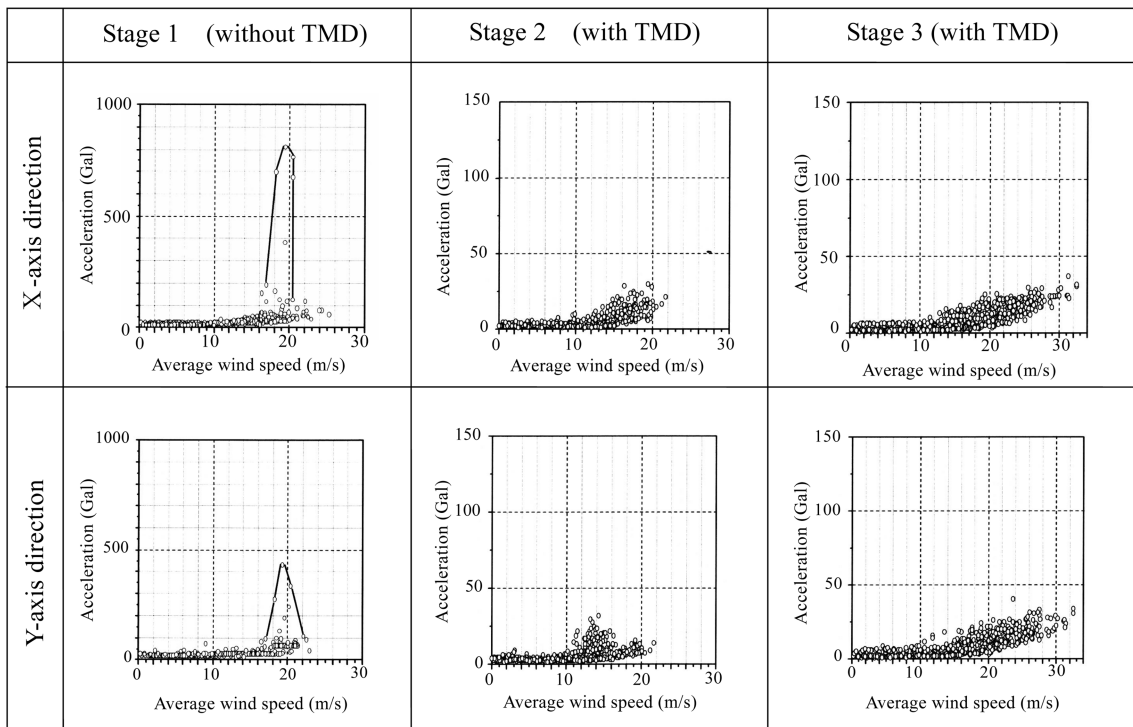


Fig. 2 Correlation between average wind speed and maximum acceleration amplitude

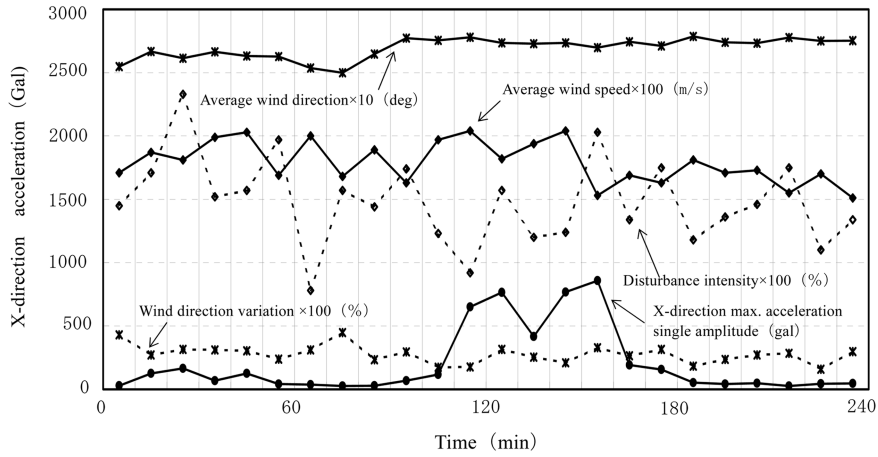


Fig. 3 10-min. data for 4 straight hours at vortex-induced vibration

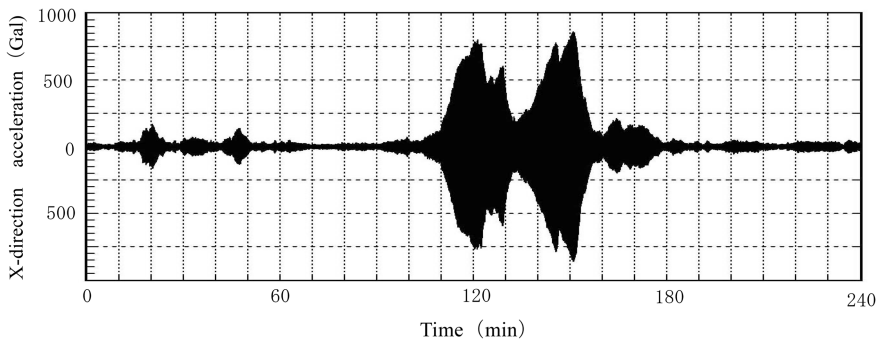


Fig. 4 X-direction acceleration time-series waveform at vortex-induced vibration

occurrence of a significant vibration acceleration, at an average wind speed of around 19 m/s, which is a resonant velocity range, in Stage 1 before TMD installation. This large vibration acceleration was not seen after the TMD installation in Stages 2 and 3.

It is said that large-scale vibrations may occur in cold climates (Hansen 1998). In fact, at Stage 1, a large vibration due to wind blowing from the sea occurred only once during the night in January 2001. To examine the resonant velocity at Stage 1 in detail, we obtained data in 10-minute blocks on the average wind speed, disturbance intensity, average wind direction, variation of wind direction, and X-direction maximum acceleration single amplitude, extending for four straight hours when the maximum vibration acceleration occurred, as shown in Fig. 3. The X-direction acceleration time-series waveform is presented in Fig. 4. The numeric values of longitudinal axis in Fig. 3 indicate indexes showing acceleration (Gal), wind direction (deg), ratio of standard deviation of wind direction variation against average wind direction (%), wind speed (m/s), and disturbance intensity (%) respectively. Such indexes are sought by multiplying each physical quantity by individual coefficients. As shown in this figure, in the repetitive increase or decrease of the amplitude, a large-scale amplitude exceeding 200 Gal emerged for 45 minutes. In the meantime, the average wind direction was westerly and the average wind speed was between 18 and 20 m/s. In particular, the average wind speed during increasing acceleration amplitudes (amplitudes between

100 and 120 minutes and between 130 and 150 minutes) stayed around 20 m/s. The disturbance intensity and the wind direction variation were relatively small values as compared to the other 10-minute blocks of data.

From these findings, it can be considered that a resonant velocity developing to a large-scale amplitude may be generated when the disturbance intensity in the resonant velocity area is less and when, concurrently, the wind direction is stable with less variation. The relationship between wind

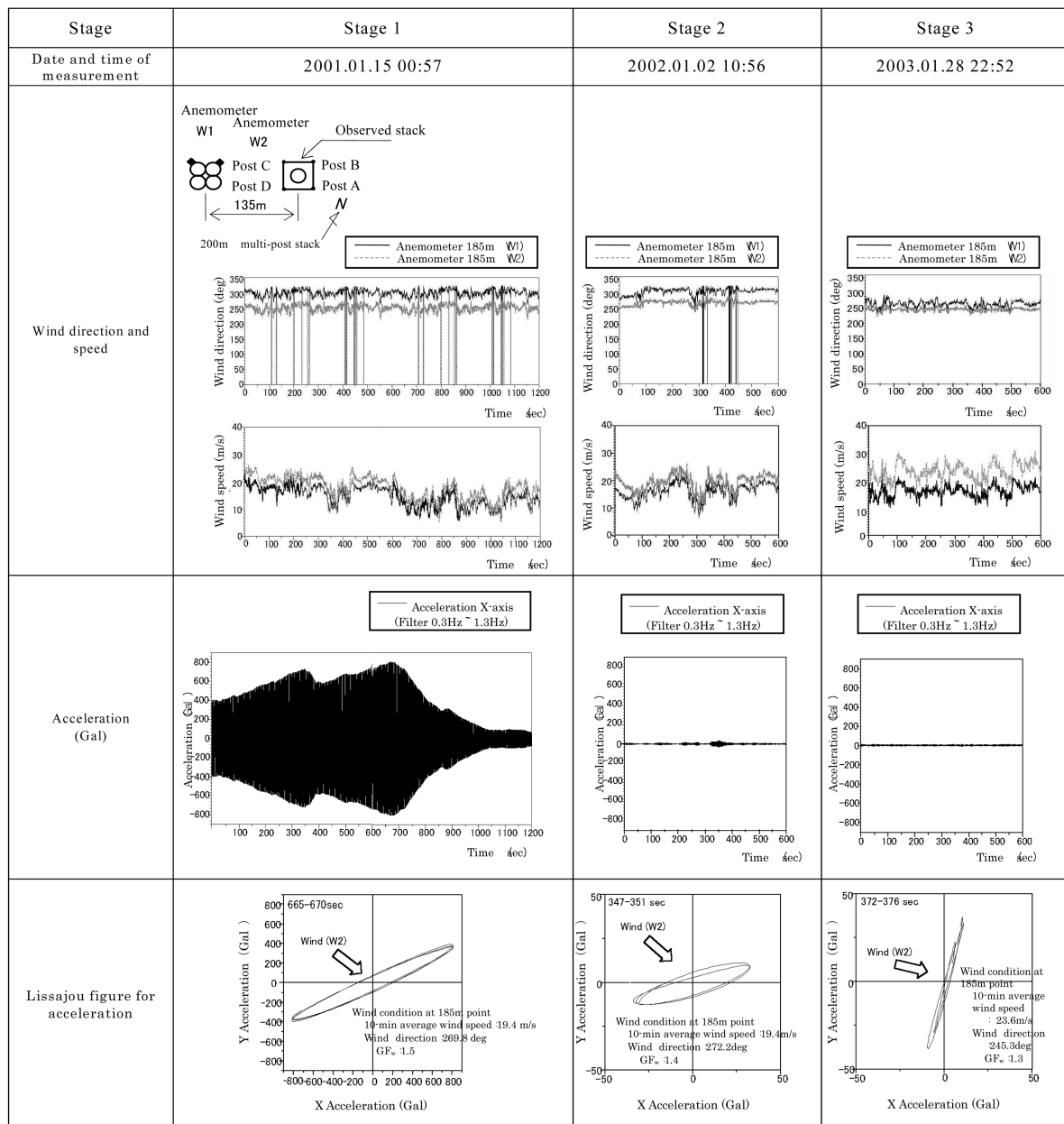


Fig. 5 10-minute time evolution and Lissajou figures for vibration acceleration

direction and speed and maximum acceleration varies even in 10 minutes; therefore, more focus should be placed on the relationship between the wind direction, speed and maximum acceleration in a shorter period of time.

Fig. 5 shows the time evolution and Lissajou figures from the time when significant vibration acceleration was observed in each stage in the resonant velocity range as shown in Table 4. The stack vibrated at a right angle against the wind direction. This suggests that the vibration in the resonant velocity range is a vortex-induced vibration attributable to the Karman vortex. The reason for the decrease in the vibration acceleration to about one-twentieth of the value in Stage 2, despite the wind conditions being similar in Stages 1 and 2, is likely to be the damping effect of the TMD. The wind speed of 19.4 m/s in Stage 1 is the average value calculated for 10 minutes until achieving the maximum acceleration. Table 5 shows the single amplitudes δ of vibration at the top of the tower. These values were calculated from the maximum acceleration value using the Lissajou figures when significant vibration acceleration occurred in each stage as obtained in Fig. 5. Here, $\delta(\text{mm})=10 \cdot A / (2\pi f)^2$, and A is the vibration acceleration (Gal) corresponding to the first natural frequency f : (Hz).

3.3. Gust response based on strain data

The average strain (ϵ_{mean}) for each post was calculated from the strain observed in the tower's post-material by strain meters installed at a height of $GL+90.5$ m. The correlation with U_{185} is shown in Fig. 6. The figure shows the data for Stage 3 in which strong winds were observed. Scattered gust response values are seen when U_{185} is 20 m/s or less; however, correlation is seen between the

Table 5 Resonance amplitude

Stage	Wind conditions		Vibration acceleration (single amplitude of vibration)
	Wind speed U_{185} (m/s)	Wind direction ($^\circ$)	
1	19.4	269.8	825 Gal (670 mm)
2	19.4	272.2	35.2 Gal (30 mm)
3	23.6	245.3	38.5 Gal (35 mm)

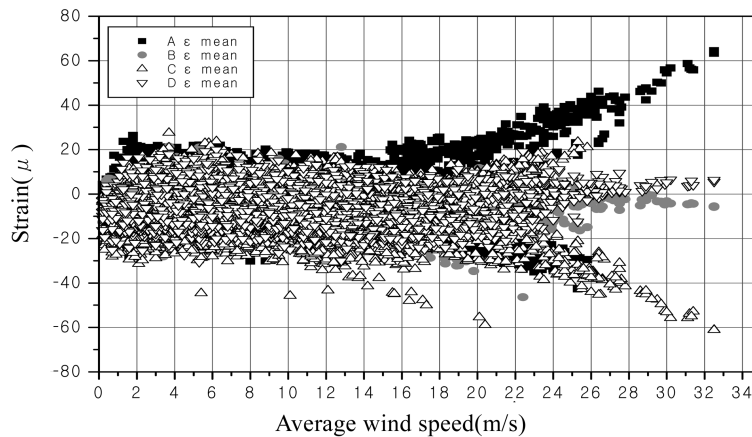


Fig. 6 Correlation between average wind speed and average strain in Stage 3

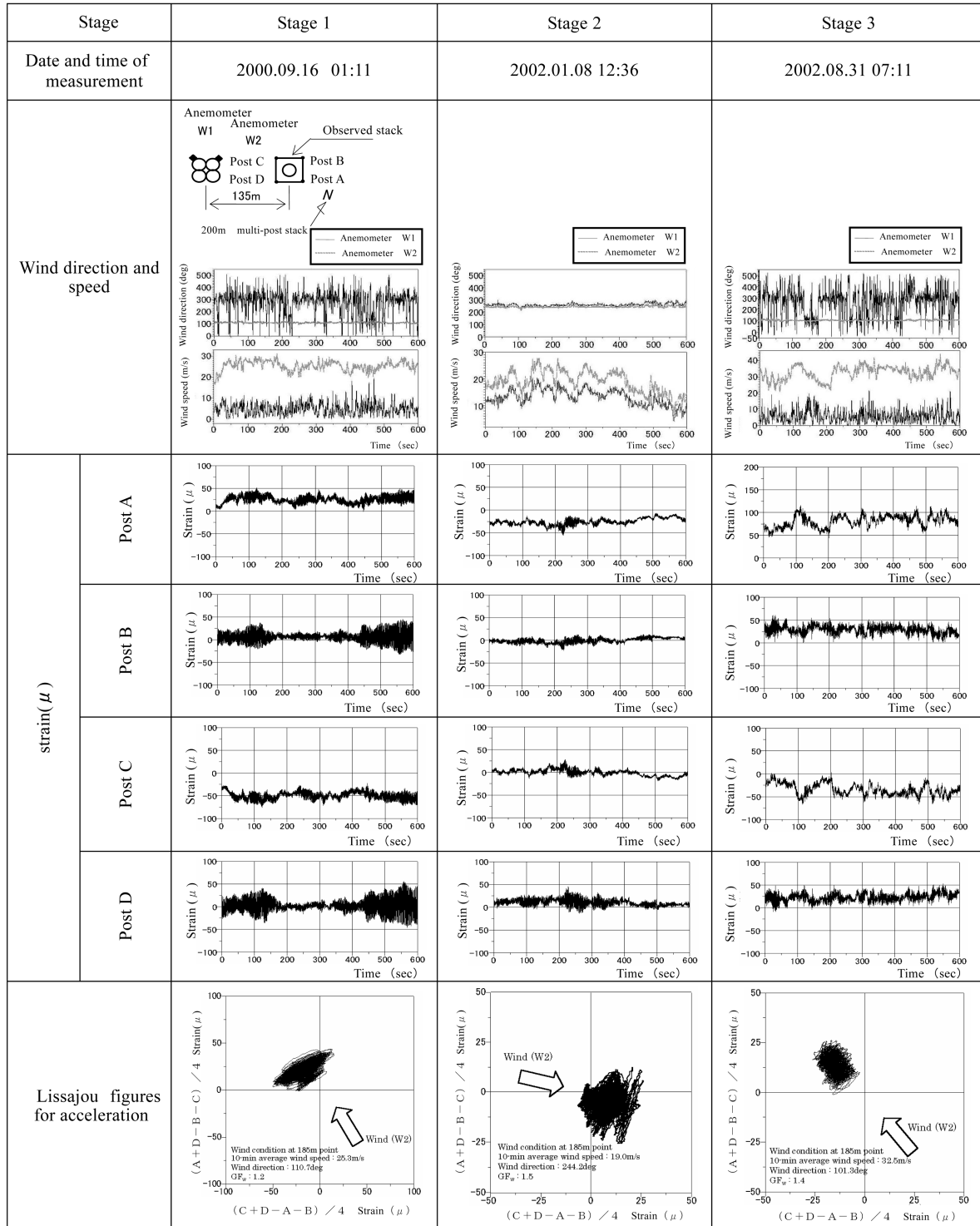


Fig. 7 10-minute time evolution and Lissajou figures for post strain

Table 6 Gust response rate

Stage	Wind conditions			GF_ε
	U_{185} (m/s)	(°)	GF_w	
1	24.3	109.8	1.3	2.14
"	24.9	246.3	1.2	1.49
"	25.3	110.7	1.2	1.58
3	29.2	101.1	1.3	1.36
"	31.3	102.0	1.3	1.32
"	32.5	102.1	1.3	1.31

wind speed and gust response value when the wind speed range is around 20 m/s or more.

Fig. 7 shows the 10-minute time evolution and Lissajou figures for post-strain experienced under strong winds for each stage. The Lissajou figures represent the behavior of the stack's gust response, which suggests that the stack vibrates while bending in the direction of strong wind.

The gust response is evaluated using the maximum strain value (ε_{\max}), average strain ($\varepsilon_{\text{mean}}$) and fluctuating strain (ε_{amp}) in the wind's direction, all of which were observed on the tower when strong winds occurred. More specifically, the gust factor of the strain is calculated as $GF_\varepsilon = (\varepsilon_{\text{mean}} + \varepsilon_{\text{amp}}) / \varepsilon_{\text{mean}}$. Table 6 shows the GF_ε in Stages 1 and 3. A tendency for the gust response to decrease as the damping ratio increases was found.

4. TMD structure and wind tunnel test

4.1. Mechanism of TMD

The installation of a TMD is shown in Fig. 8. To adjust the damping ratio, weight was controlled

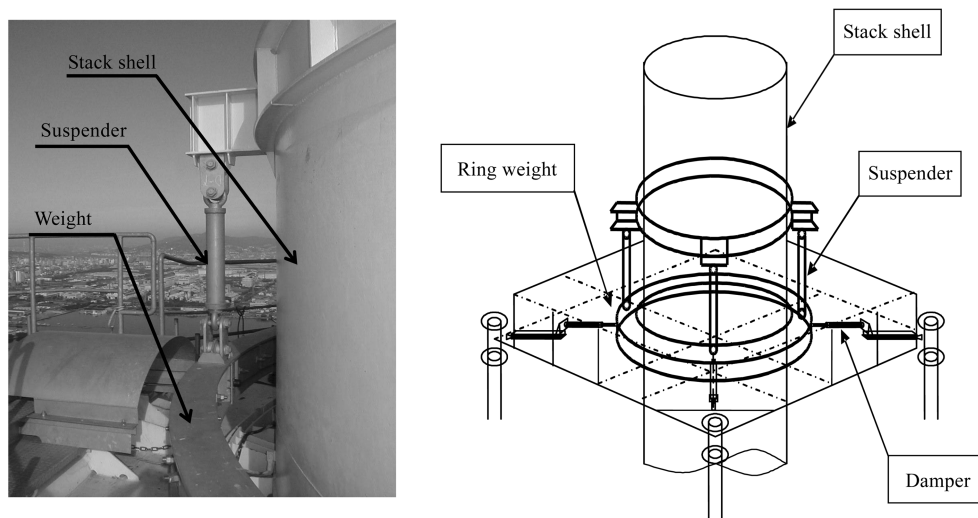


Fig. 8 TMD structure

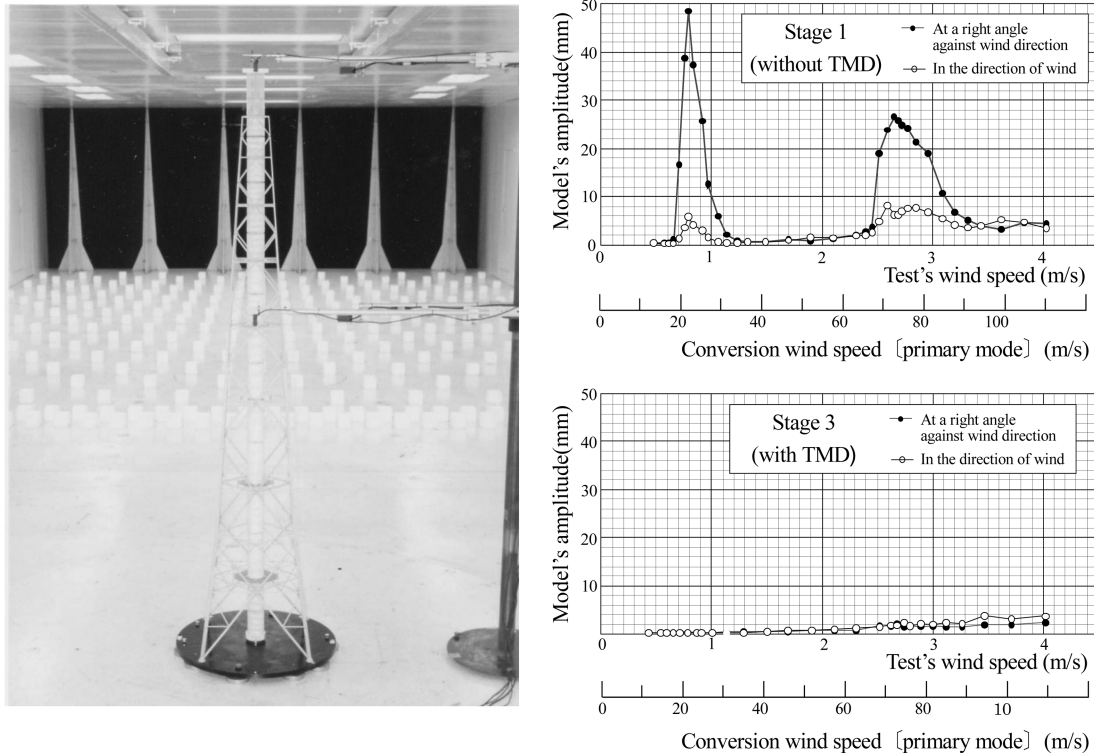


Fig. 9 Wind tunnel test

by a decrease or increase in steel materials and by using the spring constant with the length of the suspender.

4.2. Wind tunnel test

Together with the observation of the actual stack, a wind tunnel test using a model one-eightieth of the actual size was carried out to reproduce vortex-induced vibration for Stages 1 and 3, as shown Fig. 9. Judging from the test results of Stages 1 and 3, the test successfully reproduced the controlling effect of the TMD on vortex-induced vibration on the whole stack structure.

5. Conclusions

The observation data, gathered from 2000 to 2003, of a tower-supported steel stack constructed with a single-stack shell and four posts has been described. The stack's vibration properties and the characteristics of vortex-induced vibration and gust response were examined; and, the effect of the vibration control measure was confirmed. Through long-term observation, a man-powered vibration test and a wind tunnel test, the following conclusions were derived.

- (1) Vortex-induced vibration was recognized at a resonant velocity range in a tower-supported steel stack as well as a cylinder-type stack. In particular, when the intensity of wind disturbance is less, and, concurrently, the wind direction is stable, the stack's acceleration

- amplitude increases sharply in a short period of time.
- (2) The tower-supported steel stack vibrated while bending in the direction of the wind.
 - (3) By increasing the damping ratio due to the effects of TMD, the vortex-induced vibration and gust response of the tower-supported steel stack decreased. In particular, vortex-induced vibration was reduced dramatically.
 - (4) To maximize and maintain the damping effect over a long period of time, it is extremely important to optimally adjust the weight of a TMD and the length of its suspenders. In addition, finely-tuned maintenance, including regular inspections, of the TMD is also required.

References

- Architectural Institute of Japan (1996), Recommendations for Building Design Load.
- CICIND (1999), Model Code for Steel Chimneys Revision 1.
- Ciesielski, R., Gaczek, M., and Kawecki, J. (1992), "Observation results of cross-wind response of towers and steel chimneys", *J. Wind Eng. Ind. Aerodyn.*, **41-44**, 2205-2211.
- Eurocode 1 (1995), Basis of design and actions on structures.
- Hansen, S. O. (1998), "Vortex-induced vibrations of line-like structures", *Proceedings of CICIND's 50th Meeting*, Oxford, September.
- Homma, S., Susuki, T., Endou, O., Hanada, N., Ohmori, M., Makihata, T., and Maeda, J. (2004), "Vortex-induced and gust responses of a tower supported steel stack", *J. Struct. Eng.*, **50B**, 687-694 (in Japanese with an English summary).
- Homma, S., Susuki, T., Hanada, N., Maeda, J., and Ohmori, M. (2004), "Wind responses of constitutive members of a tower-supported steel stack", *Proceedings of 18th National Symposium on Wind Engineering*, Tokyo, December (in Japanese with an English summary).
- Kawamura, S. and Okazaki, M. (1999), "Full scale measurement on a rectangular tower supported stack with two flues", *Proceedings of the 10th International Conference on Wind Engineering*, Copenhagen, June.
- Kawamura, S., Kiuchi, T., and Taniguchi, T. (1992), "Full scale measurement on a triangular tower-supported stack with two flues", *J. Wind Eng. Ind. Aerodyn.*, **41-44**, 2177-2186.
- Koten, H. (1998), "Vortex excitation of steel chimneys", *Wind Effects on Buildings and Structures*, Riera & Davenport (eds.), Balkema, Rotterdam, 209-219.
- Makihata, T., Maeda, J., Tada, T., Miyajima, H., and Homma, S. (2002), "Field observations on flow-induced vibration of a tower supported steel stack", *Proceedings of 17th National Symposium on Wind Engineering*, Tokyo, December (in Japanese with an English summary).
- Sanada, S., Suzuki, M., and Matsumoto, H. (1992), "Full scale measurements of wind force acting on a 200 m concrete chimney, and the chimney's response", *J. Wind Eng. Ind. Aerodyn.*, **41-44**, 2165-2176.
- Simiu, E. and Scanlan, R. H. (1996), *Wind Effects on Structures*, 3rd Ed, John Wiley & Sons, Inc.
- Susuki, T., Hanada, N., Ohmori, M., Homma, S., and Maeda, J. (2004), "Wind-induced vibration of tower-supported steel stack", *Proceedings of The 15th Conference on Electric Power Supply Industry*, Shanghai, October.
- Tranvik, P. and Alpsten, G. (2005), "Structural behavior under wind loading of a 90 m steel chimney", *Wind and Struct., An Int. J.*, **8**(1), 61-78.
- Ueda, T., Nakagaki, R., and Koshida, K. (1992), "Suppression of wind-induced vibration by dynamic dampers in tower-like structures", *J. Wind Eng. Ind. Aerodyn.*, **41-44**, 1907-1918.
- Verwiebe, C. and Berger, G. W. (1999), "Measured damping decrements of steel chimneys and their dependence on design of the chimneys", *Proceedings of The 10th International Conference on Wind Engineering*, Copenhagen, June.
- Vickery, B. J. (1998), "Wind loads and design criteria for chimneys", *Wind Effects on Buildings and Structures*, Riera & Davenport (eds.), Balkema, Rotterdam, 273-296.